Research Article

A Geometrical-Based Model for Cochannel Interference Analysis and Capacity Estimation of CDMA Cellular Systems

Konstantinos B. Baltzis

Section of Applied and Environmental Physics, Department of Physics, Aristotle University of Thessaloniki,
54124 Thessaloniki, Greece

Correspondence should be addressed to Konstantinos B. Baltzis, kmpal@physics.auth.gr

A common assumption in cellular communications is the circular-cell approximation. In this paper, an alternative analysis based on the hexagonal shape of the cells is presented. A geometrical-based stochastic model is proposed to describe the angle of arrival of the interfering signals in the reverse link of a cellular system. Explicit closed form expressions are derived, and simulations performed exhibit the characteristics and validate the accuracy of the proposed model. Applications in the capacity estimation of WCDMA cellular networks are presented. Dependence of system capacity of the sectorization of the cells and the base station antenna radiation pattern is explored. Comparisons with data in literature validate the accuracy of the proposed model. The degree of error of the hexagonal and the circular-cell approaches has been investigated indicating the validity of the proposed model. Results have also shown that, in many cases, the two approaches give similar results when the radius of the circle equals to the hexagon inradius. A brief discussion on how the proposed technique may be applied to broadband access networks is finally made.

1. INTRODUCTION

Wireless communications become more and more popular in our daily life. This impressive evolution imposes a series of challenges. Networks are asked to deal with a multimedia traffic mix of voice, data, and video, each having different transfer requirements while demands on capacity always increase [1]. A major challenge for engineers is the development of realistic models that can efficiently estimate the performance of wireless systems. Among the various performance degradation factors, cochannel interference (CCI) is quite significant especially since cells in a cellular system tend to be denser for capacity reasons [2].

The development of models that describe CCI is of great interest nowadays. Reliable models can be found in the published literature; see, for example, [3–6]. However, their complexity and computational cost bounds their application. Nevertheless, simple geometrical-based models have been developed allowing approximate but adequate system performance estimation; see, for example, [7–11]. A

simple approach is presented in [7]. There, the estimation of the reverse link performance degradation due to CCI is based on the calculation of the probability density function (pdf) of the angle of arrival (AoA) of the interfering signals at the base station (BS). The circular-cell approximation is the main assumption of the approach, an assumption quite common in cellular systems [12]. This approximation is usually valid despite the circular cells must partially overlap in order to avoid gaps, [13]; however, in some cases it gives poor results; see, for example, [14].

In this paper, a proposal that extends the model in [7] by considering the hexagonal shape of the cells is presented. The main benefit of the proposed model is the increased accuracy comparing to [7], as well, its simplicity and low-computational cost compared to deterministic and nongeometrical models. Simple closed form expressions for the statistics of the AoA of the interfering signals in the reverse link of cellular systems, when the closest edges of two cells are properly aligned, are provided. Performance evaluation is based on the calculation of the average probability that the
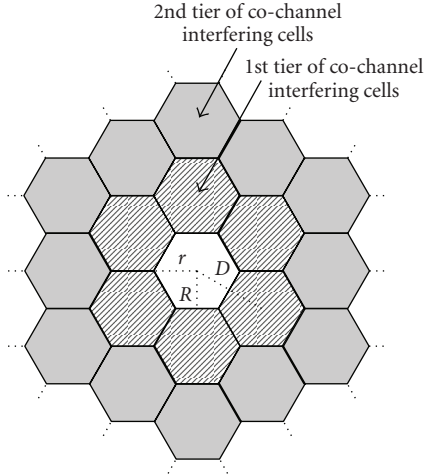
FIGURE 1: Typical hexagonal cell pattern (cluster size is one).

desired signal does not exceed CCI by a specific protection ratio (outage probability).

The paper is organized as follows. The system geometry and the assumptions made are presented in Section 2. In Section 3, the proposed model is described. Numerical examples and discussions are provided in Section 4. Concluding remarks are finally drawn in Section 5.

2. SYSTEM GEOMETRY AND MAIN ASSUMPTIONS

A cellular system hexagonal cell pattern with cluster size $K = 1$ is illustrated in Figure 1. The distance between the centers of two cochannel cells is D. The inradius and circumradius of the hexagonal cells are denoted with R and r, respectively. A single line-of-sight signal path between each interferer and the desired BS is considered. BSs are located at the centers of the cells, and the mobiles are uniformly distributed within the cells. The model assumes only the first ring of cochannel interferers. The environment is interference-limited, that is, CCI is the only limiting factor of performance [15]. For simplicity, a conventional downlink beamforming scheme (i.e., each BS main beam is aimed directly toward the desired mobile user) is assumed.

3. MATHEMATICAL FORMULATION

In the geometrical-based model proposed in [7], the cells are approximated as circles with radius ρ. The pdf of the AoA of the interfering signals in the reverse link is

$$f_c(\phi) = \frac{2D}{\pi\rho}\cos\phi\sqrt{1 - \left(\frac{D}{\rho}\right)^2\sin^2\phi} \\ \cdot U\left(\sin^{-1}\left(\frac{\rho}{D}\right) - |\phi|\right), \tag{1}$$

where $U(x)$ is the unit step function. For brevity reasons, the analysis of the circular-cell approach is not repeated. This model is extended here by considering the hexagonal shape of the cells. The analysis applied to the case when the closest
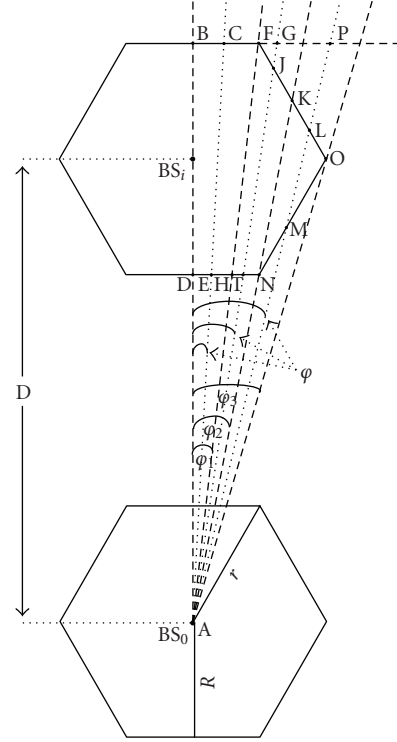

FIGURE 2: Proposed hexagonal model.

edges of two cochannel cells are properly aligned (e.g., a hexagonal structure with cluster size one, see Figure 1). Since the users are assumed to be uniformly distributed within the cell, the probability of the AoA of the interfering signals at the BS is proportional to the area $E(\phi)$ of the polygon defined from the axis that connects the BSs of the desired and the interfering cell, BS_0 and BS_i, respectively, the line segment determined from the angle ϕ, and the boundaries of the interfering cell; see Figure 2. In general, $\forall D : D \geq 2R$, three different subregions determined by the angles

$$\phi_i = \cot^{-1}\left(\frac{\sqrt{3}D}{\mu_i R} + \lambda_i\right), \quad i = 1, 2, 3 \tag{2}$$

with $\mu = \{1, 1, 2\}$ and $\lambda = \{\sqrt{3}, -\sqrt{3}, 0\}$ are defined.

Obviously, for $|\phi| \leq \phi_1$, it is

$$E_1(\phi) \equiv E(BCDE) = E(ABC) - E(ADE), \tag{3}$$

where $E(X_1 X_2 \cdots X_q)$ is the area of the q-sided polygon $X_1 X_2 \cdots X_q$. It is

$$E(ABC) = \frac{1}{2}(D + R)\overline{BC} = \frac{1}{2}(D + R)^2 \tan\phi,$$

$$E(ADE) = \frac{1}{2}(D - R)\overline{DE} = \frac{1}{2}(D - R)^2 \tan\phi, \tag{4}$$

where $\overline{X_1 X_2}$ is the length of the line segment with endpoints X_1 and X_2. It is finally

$$E_1(\phi) = 2RD \tan\phi. \tag{5}$$

For $\phi_1 \leq |\phi| \leq \phi_2$, it is

$$E_2(\phi) \equiv E(\text{FGHI})$$
$$= E(\text{ABG}) - (E_1(\phi_1) + E(\text{ADI}) + E(\text{FGJ})) \tag{6}$$

with

$$E(\text{BGA}) = \frac{1}{2}(D+R)\overline{\text{BG}} = \frac{1}{2}(D+R)^2 \tan\phi,$$
$$E(\text{ADI}) = \frac{1}{2}(D-R)\overline{\text{DI}} = \frac{1}{2}(D-R)^2 \tan\phi. \tag{7}$$

Using the angle-angle-side (AAS) theorem [16], after some manipulation we get

$$E(\text{FGJ}) = \frac{\sin(\pi/3)\sin(\pi/2 - \phi)}{2\sin(\pi/6 + \phi)}$$
$$\cdot (R+D)^2(\tan\phi - \tan\phi_1)^2. \tag{8}$$

Therefore, (6) gives

$$E_2(\phi) = 2DR(\tan\phi - \tan\phi_1)$$
$$- \frac{\sqrt{3}(D+R)^2}{2} \cdot \frac{(\tan\phi - \tan\phi_1)^2}{1 + \sqrt{3}\tan\phi}. \tag{9}$$

Similarly, for $\phi_2 \leq |\phi| \leq \phi_3$, it is

$$E_3(\phi) \equiv E(\text{KLMN})$$
$$= \frac{A}{2} - (E_1(\phi_1) + E_2(\phi_2) + E(\text{LMO})), \tag{10}$$

where $A = 2\sqrt{3}R^2$ the area of the hexagon, and

$$E(\text{LMO}) = \frac{\sin(2\pi/3)\sin(\pi/6 + \phi)}{2\sin(\pi/6 - \phi)}$$
$$\cdot \overline{\text{LO}}^2 = \frac{\sqrt{3}\sin(\pi/6 + \phi)}{4\sin(\pi/6 - \phi)}(r - \overline{\text{FL}})^2. \tag{11}$$

It is also

$$\frac{\overline{\text{FL}}}{\sin(\pi/2 - \phi)} = \frac{\overline{\text{FP}}}{\sin(\pi/6 + \phi)}$$
$$\Longrightarrow \overline{\text{FL}} = \frac{2}{1 + \sqrt{3}\tan\phi}\overline{\text{FP}} \tag{12}$$

with

$$\overline{\text{FP}} = \overline{\text{BP}} - \overline{\text{BF}} = (R+D)(\tan\phi - \tan\phi_1). \tag{13}$$

Using (10)–(13), $E_3(\phi)$ is calculated as

$$E_3(\phi) = \sqrt{3}R^2 - \left\{ E_1(\phi_1) + E_2(\phi_2) \right.$$
$$\left. + \frac{[R + \sqrt{3}(D+R)\tan\phi_1 - \sqrt{3}D\tan\phi]^2}{\sqrt{3}(1 - 3\tan^2\phi)} \right\}. \tag{14}$$

Since the users are uniformly distributed within the hexagonal cell, their density f_{area} is inversely proportional to the area of the hexagon. The cumulative distribution function (cdf) of the incoming interfering signals is given by

$$F(\phi) = f_{\text{area}}E(\phi) = \sum_{i=1}^{3} \frac{E_i(\phi)}{A}. \tag{15}$$

Differentiation of (15) gives the pdf of the AoA of the interfering signals. It is

$$f(\phi) = \begin{cases} \dfrac{D}{\sqrt{3}R}\sec^2\phi, & |\phi| \leq \phi_1, \\[2mm] \left\{ \begin{aligned} &\dfrac{D}{\sqrt{3}R} - \dfrac{1}{4}\left(1 + \dfrac{D}{R}\right)^2 \\ &\times \dfrac{(\tan|\phi| - \tan\phi_1)}{(1 + \sqrt{3}\tan|\phi|)^2} \\ &\times [2 + \sqrt{3}(\tan|\phi| + \tan\phi_1)] \end{aligned} \right\} \cdot \sec^2\phi, \\ & \phi_1 \leq |\phi| \leq \phi_2, \\[2mm] -\dfrac{[R + \sqrt{3}(D+R)\tan\phi_1 - \sqrt{3}D\tan|\phi|]}{\sqrt{3}[R(1 - 3\tan^2\phi)]^2} \\ \times \{-D + \sqrt{3}[R + \sqrt{3}(D+R)\tan\phi_1] \\ \times \tan|\phi|\} \cdot \sec^2\phi, & \phi_2 \leq |\phi| \leq \phi_3, \\ 0, & |\phi| > \phi_3 \end{cases} \tag{16}$$

for any $D > 2R$. When $D = 2R$ (or equivalently $K = 1$), (16) is simplified into

$$f(\phi) = \begin{cases} \dfrac{2}{\sqrt{3}}\sec^2\phi, & |\phi| \leq \tan^{-1}\left(\dfrac{1}{3\sqrt{3}}\right), \\[2mm] \left\{ \begin{aligned} &\dfrac{2}{\sqrt{3}} - \dfrac{9}{4}\dfrac{(\tan|\phi| - \tan\phi_1)}{(1 + \sqrt{3}\tan|\phi|)^2} \\ &\times [2 + \sqrt{3}(\tan|\phi| + \tan\phi_1)] \end{aligned} \right\} \cdot \sec^2\phi, \\ & \tan^{-1}\left(\dfrac{1}{3\sqrt{3}}\right) \leq |\phi| \leq \dfrac{\pi}{6}, \\ 0, & |\phi| > \dfrac{\pi}{6}. \end{cases} \tag{17}$$

For a given ϕ, the probability that a particular user is causing interference is

$$P(\phi) = G(\phi) \otimes f(\phi), \tag{18}$$

where $G(\phi)$ is the desired BS antenna radiation pattern, and $\otimes$ is the convolution operator. The average probability of outage of CCI is [7]

$$P(\text{outage}) \underset{\text{def}}{=} P(\text{CIR} < \gamma)$$
$$= \sum_{n=1}^{N} P(Z_d < 0 \mid n)P(n), \tag{19}$$

where CIR is the carrier to interference ratio (CIR), $P(n)$ is the average probability over ϕ that n out of the possible N interfering cells are causing interference, γ is the protection ratio, Z_d is the carrier to interference plus protection ratio (CIPR), and $P(Z_d < 0 \mid n)$ is the conditional probability of outage given n interferers assuming combined Rayleigh and Lognormal fading [7, 8].

4. NUMERICAL RESULTS AND DISCUSSIONS

In this Section, results of the numerical evaluation of the proposed model are presented. The accuracy of the proposed model and the circular-cell approximation is examined in detail. The impact of the BS antenna radiation pattern and the sectorization of the cells on the reverse link performance of a WCDMA cellular system are also investigated.

The first two sets of results presented are the pdfs and the cdfs of the AoA of the interfering signals at the desired BS. Using (1), (16), and (17), the pdfs for cellular systems with $D = 2R$ (typical value for WCDMA systems) and $D = 5R$ are evaluated for both the proposed model and the circular-cell approximation and presented in Figure 3. In the circular-cell approximation, cell radius is equal to the inradius ($\rho = R$) or to the circumradius ($\rho = r$) of the hexagonal cell. For brevity reasons, they will be mentioned as inradius and circumradius approximation (approach), respectively. There are significant differences in the curves for $\phi \cong 0$ and great values of ϕ. The inradius approximation gives results closer to the hexagonal-cell approach. Note that $\arg\max_\phi f(\phi) \neq 0$, that is, the argument of the maximum of $f_c(\phi)$. It easily comes that $\forall D : D \geq 2R$ the absolute relative difference in the pdf value at $\phi = 0$ between the circular-cell approximation and the proposed model is 4.7% if $\rho = R$, and 10.3% when $\rho = r$. Integrating (1), (16), and (17), the corresponding cdfs are calculated and illustrated in Figure 4. Noticeable differences are observed between the three approaches. Again, the inradius approximation gives results closer to the hexagonal-cell approach.

The probability that an interfering cell is causing interference over ϕ is illustrated in Figure 5. Two WCDMA cellular systems have been considered. In the first case, six-sectored cells using directional antennas with half-power beamwidth HP = 65° are used. In the second, a narrow beam BS antenna (HP = 10°) is assumed. In both cases, BS antenna radiation patterns are in the form of cosϕ with sidelobe level −15 dB, typical measured values for WCDMA networks [17, 18]. As ϕ approaches zero differences are observed, mainly in the narrow beam system ($P(\phi)$ in the proposed model is smaller about 7% and 21% compared to the inradius and the circumradius approaches, resp.). Differences are also observed at angles point at the edges of the interfering cell. However, in the six-sectored configuration, the inradius approximation gives adequate results. It may also be concluded, due to lower probability of interference, that performance degradation due to CCI is smaller in the narrow beam system compared to the six-sectored one.

Moreover, the calculated values of pdfs and cdfs show the differences between the proposed model and the circular-cell approximations. Noticeable differences are observed at
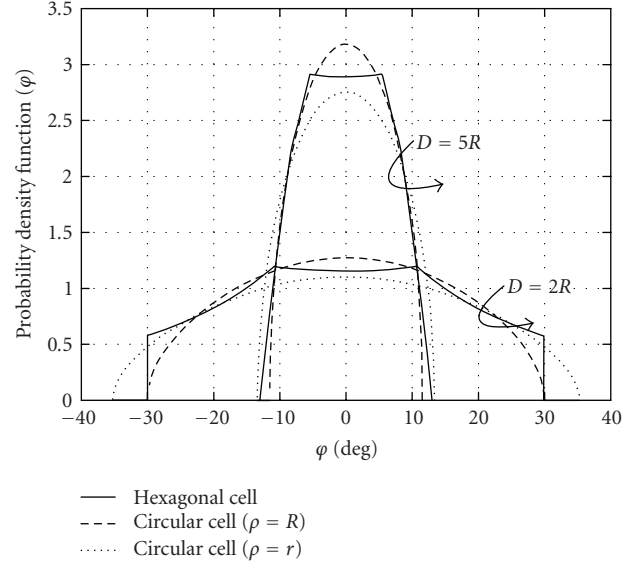

Figure 3: Pdf of the AoA of the interfering signals at the desired base station.
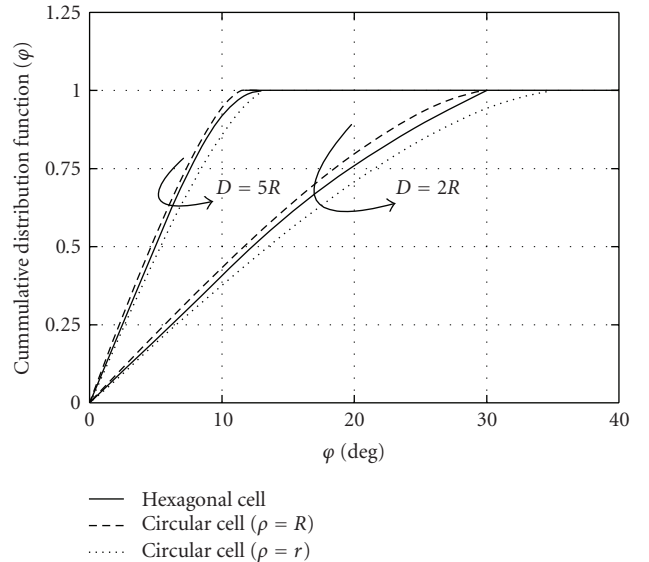

Figure 4: Cdf of the AoA of the interfering signals at the desired base station.

small angles and at $\Phi \cong \sin^{-1}(P/D)$. However, in narrow beam systems, significant differences are observed in the calculation of the probability of interference also.

In order to validate the accuracy and reliability of the models, simulation results are presented. The pdfs in (1) and (17) are evaluated for a test case of a single cluster size WCDMA system. Shadow fading is modeled as an independent log-normally distributed multiplicative noise on the signal strength received from the BS combining Rayleigh and Lognormal fading [7, 8]. Users density function is defined as in [19]. Reverse link chip rate is 3.84 Mchips/ sec. Rest of the
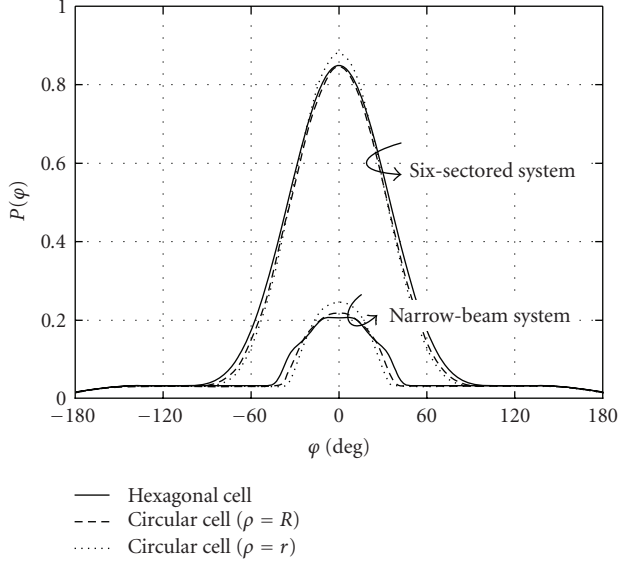
FIGURE 5: Probability that an interfering cell is causing interference over ϕ.

TABLE 1: Pdfs values: simulated estimation errors.

Hexagonal model		Circular model			
		$\rho = R$		$\rho = r$	
$\langle e_f \rangle$	$\langle \varepsilon_f \rangle$	$\langle e_f \rangle$	$\langle \varepsilon_f \rangle$	$\langle e_f \rangle$	$\langle \varepsilon_f \rangle$
1.48%	1.87%	8.17%	10.40%	9.76%	20.36%

system parameters is similar to the ones in [20]. In Table 1, the mean absolute estimation error defined as

$$\langle e_f \rangle = \frac{1}{N} \sum_{i=1}^{N} | f_{\text{sim}}^{[i]} - f^{[i]} | \qquad (20)$$

and the mean relative estimation error given from

$$\langle \varepsilon_f \rangle = \frac{1}{N} \sum_{i=1}^{N} \left| \frac{f_{\text{sim}}^{[i]} - f^{[i]}}{f_{\text{sim}}^{[i]}} \right| \qquad (21)$$

are presented. With $f^{[i]}$ is denoted the analytically derived pdf and with $f_{\text{sim}}^{[i]}$ its simulated value. Results are calculated by carrying out 1000 Monte Carlo trials. The simulated results closely match the theoretical pdf of (17). On the other hand, significant differences are observed between the simulated and the circular-cell approximations results. It has to be mentioned that the inradius approximation gives results closer to the simulated values.

In Table 2, the simulated and the analytically derived results of (1), (17), and (18) are compared. Two system architectures, the six-sectored and the narrow beam one (details are given in previous paragraph), are considered. The rest of the system parameters are as previously defined. The mean absolute, $\langle e_P \rangle$, and the mean relative, $\langle \varepsilon_P \rangle$, estimation errors are defined from (20) and (21) substituting $f^{[i]}$ and $f_{\text{sim}}^{[i]}$ with $P^{[i]}$ and $P_{\text{sim}}^{[i]}$, that is, the values of probability of interference that respond to ith snapshot of the analytically
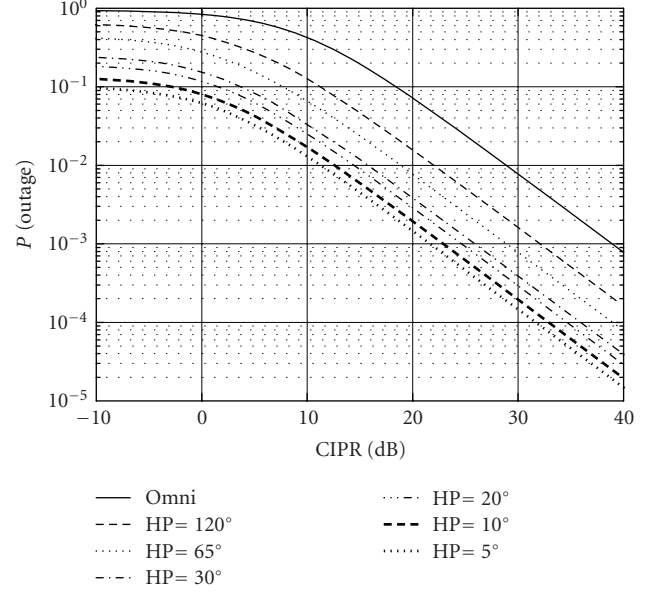

FIGURE 6: Plot of outage curves as a function of CIPR for flattop beamformers of various beamwidths. The outage curve of an omnidirectional antenna is also presented.

derived and the simulated probability, respectively. In the six-sectored network, a good agreement is observed between the theoretical and the simulated results for all models. However, in the narrow beam configuration, significant differences are found. The worst results are obtained with the circumradius approximation.

Next, the dependence of a WCDMA system performance on the BS antenna radiation pattern characteristics and the cells sectorization is investigated. Without loss of generality, the users activity level and the protection ratio are assumed $P = .4$ and $\gamma = 8$ dB. The outage curves as a function of CIPR are shown in Figure 6. In the simulations, the mobile's signal is received by flattop beamformers of various beamwidths or an omnidirectional BS antenna. Decrease in the beamformer's beamwidth up to a point reduces significantly the outage probability of CCI, indicating the improved performance obtained by sectorization and the use of narrow beam antennas. Typical values of CIR at the input of the receiver in the reverse link of a WCDMA system are usually close to 7 dB [21, 22]. The maximum acceptable outage probability is set at 10^{-2} for voice and video transmission, and 10^{-3} for web browsing and data [23]. As shown in Figure 6, voice and video transmission is possible when beamformers with beamwidths lower than 20 degrees are used. However, model predictions about web browsing and data transmission are pessimistic.

In Figure 7, the relative gains between systems with different BS antenna radiation patterns are presented. The relative gain is defined as

$$\text{Relative gain (dB)} = \text{CIPR}_1 - \text{CIPR}_2, \qquad (22)$$

where $\text{CIPR}_{1(2)}$ are the CIRPs for two systems with the same outage probability. An omnidirectional antenna and

TABLE 2: Probability of interference values: simulated estimation errors.

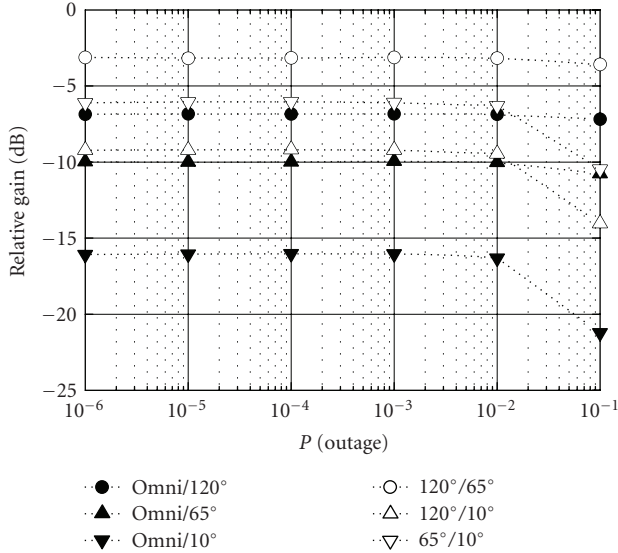| System architecture	Hexagonal model		Circular model			
			$\rho = R$		$\rho = r$	
	$\langle e_P \rangle$	$\langle \varepsilon_P \rangle$	$\langle e_P \rangle$	$\langle \varepsilon_P \rangle$	$\langle e_P \rangle$	$\langle \varepsilon_P \rangle$
Six-sectored system	0.59%	1.18%	1.34%	2.03%	1.86%	2.54%
Narrow beam system	0.47%	2.51%	1.19%	5.77%	3.99%	19.35%

FIGURE 7: Relative gain versus P (outage) for flat-top beamformers of various beamwidths. The case of an omni-directional antenna is also considered.

flattop beamformers with beamwidths equal to 120, 65, and 10 degrees are considered. Beamwidth reduction improves significantly system performance. Also, notice that the relative gain is constant for outage probabilities smaller than 1%. Assuming that CIR is approximately reciprocal to the maximum number of users [21], it can be shown that the ratio of the maximum number of users in the two systems is given by

$$\Lambda \cong 10^{-\text{Relative gain (dB)}/10}. \tag{23}$$

For example, from Figure 7, it can be shown, using (23), that the maximum number of users allowed in a six-sectored cell to the ones in a system with an omnidirectional antenna is almost five times greater ($\Lambda \cong 4.8 \sim 4.9$). Capacity in terms of the maximum number of users allowed is doubled when using a narrow beam beamformer with beamwidth equal to 10 degrees. Similar results are derived from Figure 6 in [22] for multirate single cell CDMA wireless local loop systems. As a further example, let us consider [8, Figure 4]. When $D = 2R$, the ratio of outage probabilities between two systems with BS antennas beamwidths 10 and 20 degrees and SLL = −10 dB is almost 1.3. From Figure 6 and beamformers with similar beamwidths, this ratio takes the same value (for CIPR that gives outage probability close to 10%).

A major advantage of the proposed model is its low-computational cost. In general, geometrically-based models used for the description of CCI are determined by the users' distribution within the cell. In a stochastic model, such as the one proposed here, the users positions are chosen stochastically according to a certain probability distribution. Similar models are also used in propagation channel modeling; see, for example, [24]. Advantages of these models are the physical insight they provide and their low computational cost. In general, the results they provide are adequate if one considers their reduced complexity.

This paper refers to WCDMA networks; however, the analysis presented here is valid for any single cluster size system (or for cellular geometries, where the closest edges of the two cells are properly aligned), for example, the OFDMA (WiMAX) systems or even the ad hoc networks [1, 25, 26]. Especially in MIMO-OFDM, the single cluster size networks may be loaded much further than other architectures [27]. In WiMAX systems, resources are allocated on both time and frequency bases and adjacent cells using subcarriers of exactly the same frequency and time cause interference that takes the form of collisions [28]. A suggestion on how the technique can be applied to these systems involves an extension of the model in the time domain. A simple idea may consider a joint pdf $f(\phi, \tau) = f_\phi(\phi) f_\tau(\tau \mid \phi)$, where $f_\phi(\phi)$ is given from (17), and $f_\tau(\tau \mid \phi)$ is the conditional pdf of τ for a given ϕ associated with the probability of collisions in a subcarrier [29].

5. CONCLUSIONS

In this paper, a geometrical-based model is proposed to describe the cochannel interference in a cellular system when the cluster size is one or the closest edges of two cells are properly aligned. The model considers the hexagonal shape of the cells. It is applied for the study of performance degradation due to CCI and capacity estimation of the reverse link of single cluster size systems. Analytically derived closed form expressions that provide the statistics of the AoA of the interfering signals at the BS have been provided. Model characteristics and comparisons with the circular-cell approach are presented. Simulations performed have validated the accuracy of the model. In many cases, the results derived from the hexagonal model and the inradius circular approach were similar. The dependence of the capacity of a WCDMA network on cells sectorization and BS antenna radiation pattern has also been studied. Cells sectorization and use of narrow beam BS antennas increase

significantly the capacity of a cellular system. Suggestions on how the technique can be applied to WiMAX systems are finally made.

REFERENCES

[1] W. Webb, *Wireless Communications: The Future*, John Wiley & Sons, Chichester, UK, 2007.

[2] P. Stavroulakis, *Interference Analysis and Reduction for Wireless Systems*, Artech House, Norwood, Mass, USA, 2003.

[3] S. J. Grant and J. K. Cavers, "System-wide capacity increase for narrowband cellular systems through multiuser detection and base station diversity arrays," *IEEE Transactions on Wireless Communications*, vol. 3, no. 6, pp. 2072–2082, 2004.

[4] A. Masmoudi and S. Tabbane, "Other-cell-interference factor distribution model in downlink WCDMA systems," *Wireless Personal Communications*, vol. 36, no. 3, pp. 245–275, 2006.

[5] S. Venkatesan, "Coordinating base stations for greater uplink spectral efficiency in a cellular network," in *Proceedings of the 18th International Symposium on Personal, Indoor and Mobile Radio Communications (PIMRC '07)*, pp. 1–5, Athens, Greece, September 2007.

[6] S. Karimifar and J. K. Cavers, "Achieving high-capacity narrowband cellular systems by means of multicell nultiuser detection," *IEEE Transactions on Vehicular Technology*, vol. 57, no. 2, pp. 945–953, 2008.

[7] P. Petrus, R. B. Ertel, and J. H. Reed, "Capacity enhancement using adaptive arrays in an AMPS system," *IEEE Transactions on Vehicular Technology*, vol. 47, no. 3, pp. 717–727, 1998.

[8] W. S. Au, R. D. Murch, and C. T. Lea, "Comparison between the spectral efficiency of SDMA systems and sectorized systems," *Wireless Personal Communications*, vol. 16, no. 1, pp. 51–67, 2001.

[9] Z. Zufan, W. Shihong, Y. Jing, and Z. Lianxiang, "CIR performance analysis and optimization of a new mobile communication cellular configuration," in *Proceedings of the 4th International Conference on Microwave and Millimeter Wave Technology (ICMMT '04)*, pp. 826–829, Beijing, China, August 2004.

[10] Z. Zufan, L. Fang, and D. Huiping, "More realistic analysis of co-channel interference in sectorization cellular communications systems with Rayleigh fading environment," in *Proceedings of the 2nd International Conference on Wireless Communications, Networking and Mobile Computing (WiCOM '06)*, pp. 1–5, Wuhan, China, September 2006.

[11] A. D. Panagopoulos, T. D. Kritikos, and J. D. Kanellopoulos, "Adaptive uplink power control in adjacent DVB-RCS networks: interference statistical distribution," in *Proceedings of the 18th International Symposium on Personal, Indoor and Mobile Radio Communications (PIMRC '07)*, pp. 1–4, Athens, Greece, September 2007.

[12] A. Goldsmith, *Wireless Communications*, Cambridge University Press, New York, NY, USA, 2005.

[13] S. Jivkova and M. Kavehrad, "Transceiver design concept for cellular and multispot diffusing regimes of transmission," *EURASIP Journal on Wireless Communications and Networking*, vol. 2005, no. 1, pp. 30–38, 2005.

[14] S. W. Oh and K. H. Li, "Evaluation of forward-link performance in cellular DS-CDMA with Rayleigh fading and power control," *International Journal of Communication Systems*, vol. 14, no. 3, pp. 243–250, 2001.

[15] N. C. Sagias, "Closed-form analysis of equal-gain diversity in wireless radio networks," *IEEE Transactions on Vehicular Technology*, vol. 56, no. 1, pp. 173–182, 2007.

[16] E. W. Weisstein, *CRC Concise Encyclopedia of Mathematics*, Chapman & Hall/CRC, Boca Raton, Fla, USA, 2nd edition, 2002.

[17] L. E. Bråten, M. Pettersen, and A. Spilling, "An evaluation of adaptive arrays for a UMTS FDD network deployed in a suburban area of Norway," in *Proceedings of the 14th IEEE International Symposium on Personal, Indoor and Mobile Radio Communications (PIMRC '03)*, vol. 3, pp. 2353–2357, Beijing, China, 2003.

[18] J. Niemelä, T. Isotalo, and J. Lempiäinen, "Optimum antenna downtilt angles for macrocellular WCDMA network," *EURASIP Journal on Wireless Communications and Networking*, vol. 2005, no. 5, pp. 816–827, 2005.

[19] M. Jordan, M. Senst, Y. Cui, G. Ascheid, and H. Meyr, "Downlink based intercell time synchronization using maximum likelihood estimation," in *Proceedings of the 16th IST Mobile and Wireless Communications Summit, Mediterranean Microwave Symposium*, pp. 1–5, Budapest, Hungary, July 2007.

[20] I. A. Aldmour, K. Al-Begain, and A. I. Zreikat, "Uplink capacity/coverage analysis of WCDMA with switched beam smart antennae," *Wireless Personal Communications*, vol. 43, no. 4, pp. 1705–1715, 2007.

[21] K. S. Gilhousen, I. M. Jacobs, R. Padovani, A. J. Viterbi, L. A. Weaver Jr., and C. E. Wheatley III, "On the capacity of a cellular CDMA system," *IEEE Transactions on Vehicular Technology*, vol. 40, no. 2, pp. 303–312, 1991.

[22] Y. Zhou, F. Chin, Y.-C. Liang, and C.-C. Ko, "Capacity of multirate multicell CDMA wireless local loop system with narrowbeam antenna and SINR based power control," *International Journal of Wireless Information Networks*, vol. 8, no. 2, pp. 99–108, 2001.

[23] C. Nie, T. C. Wong, and Y. H. Chew, "Outage analysis for multi-connection multiclass services in the uplink of wideband CDMA cellular mobile networks," in *Proceedings of the 3rd International IFIP-TC6 Networking Conference (NETWORKING '04)*, vol. 3042 of *Lecture Notes in Computer Science*, pp. 1426–1432, Athens, Greece, May 2004.

[24] P. Almers, E. Bonek, A. Burr, et al., "Survey of channel and radio propagation models for wireless MIMO systems," *EURASIP Journal on Wireless Communications and Networking*, vol. 2007, Article ID 19070, 19 pages, 2007.

[25] K. Lu, Y. Qian, H.-H. Chen, and S. Fu, "WiMAX networks: from access to service platform," *IEEE Network*, vol. 22, no. 3, pp. 38–45, 2008.

[26] J. G. Andrews, S. Weber, and M. Haenggi, "Ad hoc networks: to spread or not to spread? [Ad hoc and sensor networks]," *IEEE Communications Magazine*, vol. 45, no. 12, pp. 84–91, 2007.

[27] A. Tölli and M. Juntti, "System level evaluation of space-time coded MIMO-OFDM for wide area communications," in *Proceedings of the 14th IST Mobile & Wireless Communications Summit*, pp. 1–5, Dresden, Germany, June 2005, paper 240.

[28] C. Tarhini and T. Chahed, "On capacity of OFDMA-based IEEE802.16 WiMAX including adaptive modulation and coding (AMC) and inter-cell interference," in *Proceedings of the 15th IEEE Workshop on Local and Metropolitan Area Networks (LANMAN '07)*, pp. 139–144, Princeton, NJ, USA, June 2007.

[29] L. Sartori, S.-E. Elayoubi, B. Fourestié, and Z. Nouir, "On the WiMAX and HSDPA coexistence," in *Proceedings of the IEEE International Conference on Communications (ICC '07)*, pp. 5636–5641, Glasgow, Scotland, June 2007.